Liver transplantation in man: morphometric analysis of the parenchymal alterations following cold ischaemia and warm ischaemia/reperfusion

LAURA VIZZOTTO[1], MAURIZIO VERTEMATI[1], CARLO TOMMASINI DEGNA[2] AND PAOLO ASENI[3]

[1] *Dipartimento di Anatomia Umana, Milano,* [2] *Dipartimento di Chirurgia, Ospedale 'F. Villa', and* [3] *Centro Trapianti Fegato-Rene-Pancreas, Ospedale Niguarda, Milano, Italy*

(*Accepted 16 January 2001*)

ABSTRACT

Ischaemia and reperfusion phases represent critical events during liver transplantation. The purpose of this study was to describe morphological alterations of both vascular and parenchymal compartments after ischaemia and reperfusion and to evaluate the possible relationship between morphometric parameters and biochemical/clinical data. Three needle biopsies were drawn from 20 patients who underwent orthotopic liver transplantation. The first biopsy was taken before flushing with preservation solution, and the second and the third to evaluate respectively the effects of cold ischaemia and of warm ischaemia/reperfusion. Biopsies were examined by an image analyser and morphometric parameters related to the liver parenchyma were evaluated. At the second biopsy we observed a decrease of the endothelium volume fraction while the same parameter referred to the sinusoidal lumen achieved a peak value. The hepatocytes showed a lower surface parenchymal/vascular sides ratio. This parameter was reversed at the end of the reperfusion phase; furthermore the third biopsy revealed endothelial swelling and a decreased volume fraction of the sinusoidal lumen. The results quantify the damage to the sinusoidal bed which, as already known, is one of the main targets of cold ischaemia; warm ischaemia and reperfusion accentuate endothelial damage. The end of transplantation is characterised by damage chiefly to parenchymal cells. Hepatocytes show a rearrangement of their surface sides, probably related to the alterations of the sinusoidal bed. In addition, the fluctuations of morphometric parameters during ischaemia/reperfusion correlate positively with biochemical data and clinical course of the patients.

Key words: Morphometry; liver transplantation; image analysis; ischaemia; reperfusion.

INTRODUCTION

Cold storage and reperfusion both represent important factors affecting liver function after transplantation (Clavien et al. 1992; Grace, 1994). Cold ischaemia injury is the consequence of a remarkable decay of hepatocyte mitochondrial function which, at least in part, is related to the conversion of xanthine dehydrogenase to the oxidase form leading to free radicals production (McCord, 1985; Engerson et al. 1987; Reilly & Bulkley, 1990; Cutrin et al. 1996).

Warm ischaemia accentuates the damage to sinusoidal endothelial cells and to parenchymal cells. Paradoxically, the reintroduction of warm oxygenated blood in ischaemic tissue results in further cellular injury and causes a burst of free radical production and of proinflammatory cytokines.

The microvascular impairment (deterioration of sinusoidal endothelial cells and sinusoidal narrowing) observed during ischaemia/reperfusion leads to a cascade of biochemical events, such as neutrophil chemotaxis, intravascular coagulation and Kupffer cells activation (Jaeschke, 1991; Jaeschke & Farhood, 1991; Mueller et al. 1996; Scoazec et al. 1997). Commercial University of Wisconsin solution (UW), eventually enriched with free radicals scavengers, antioxidants and calcium blockers, has been used to extend the limits of preservation for liver and other

Correspondence to Prof. Laura Vizzotto, Dipartimento di Anatomia Umana, Università degli Studi di Milano, Via Mangiagalli 31, 20133 Milano, Italy. Tel.: +39 02 70646240, +39 02 38210294; fax: +39 02 38210298.

solid organs (Kalayoglu et al. 1988; Southard et al. 1990; Karwinski et al. 1996).

Because of the strictly anatomical connections between parenchymal and vascular compartments, these biochemical events are responsible for functional and structural alterations both to endothelium and to the hepatocytes. Endothelial swelling, hepatic microvasculature impairment and hepatocyte necrosis have been described. However, quantitation of the morphological features during cold ischaemia and warm ischaemia/reperfusion on the hepatic architecture, i.e. sinusoids and parenchymal compartment, has not yet been investigated.

To describe the morphological alterations in hepatic ischaemia/reperfusion (I/R), we have applied a computerised morphometric model to human liver transplantation. In addition, different biochemical and clinical parameters describing liver function both during the transplant procedure and the first week after liver transplantation have been recorded.

MATERIALS AND METHODS

Twenty cases were randomly selected among patients who underwent orthotopic liver transplantation (OLT) at the Department of Surgery 'Pizzamiglio II', Niguarda Hospital, Milan. Informed consent was obtained from each patient included in the study. The study was approved by the Institution's Human Research Committee. The age range was 34 to 55 y and the male/female ratio 15:5. No marginal donor was involved in the protocol. The age range of the donors (19 males, 1 female) was 16 to 58 y; causes of death were cerebral trauma (5) and cerebral haemorrhage (15). All donor livers were preserved and flushed with UW solution at 4 °C. The abbreviations used are listed in Table 1.

Three needle liver biopsy specimens were obtained at different time points: the first (T1) immediately before liver perfusion with UW solution: the second (T2) on the perfused liver with UW at 4 °C at the maximum of cold ischaemia time (cold ischaemia span, mean $\pm$ S.D., 7.31 ± 2.51 h); the third (T3) to evaluate the effects of warm ischaemia and reperfusion on liver structure when blood flow was re-established (warm ischaemia/reperfusion span, mean $\pm$ S.D., 2.75 ± 1.15 h).

Biopsy specimens were immediately fixed in 0.12 M phosphate buffered 3% glutaraldehyde at 20 °C, post-fixed in 1.5% OsO_4, dehydrated in acetone and embedded in Araldite. Only 1 biopsy for each time point was taken because of the potential risks related to this technique during OLT. All sampling steps follow the suggestions aimed to make a single needle biopsy of the liver sufficient for accurate morphometric analysis (Hess et al. 1973). Each biopsy was subdivided into 5 tissue blocks to avoid misinterpretation caused by intralobular differences in parenchyma characteristics. From each block, a single 1 μm section was randomly cut by a Reichert ultramicrotome and stained with toluidine blue. In this way unbiased sampling was assured (Oberholzer & Rohr, 1983). The morphometric analysis has been performed at 2 magnifications ($\times 290$, $\times 1170$), using

Table 1. *Abbreviations used*

$\bar{d}_{hep}$	mean hepatocyte diameter (μm)
$\bar{d}_{nuc}$	mean hepatocyte nucleus diameter (μm)
N/C	hepatocyte nucleus/cytoplasm mean ratio
N_v	number in unit volume (1 mm^3) of hepatocyte nuclei (as representative of mean number of mononucleated hepatocytes)
$S_v$par	surface density (mm^2 in 1 mm^3 of parenchyma) of hepatocyte parenchymal sides
$S_v$sin	surface density (mm^2 in 1 mm^3 of parenchyma) of sinusoidal bed
$S_v$vas	surface density (mm^2 in 1 mm^3 of parenchyma) of hepatocyte vascular sides
T1	time point corresponding to the beginning of cold ischaemia
T2	time point corresponding to the end of cold ischaemia and the beginning of warm ischaemia; actually, the beginning of the transplant
T3	time point corresponding to the end of warm ischaemia/reperfusion;
UW	the preservation solution 'University of Wisconsin'
OLT	orthotopic liver transplantation
$\bar{V}$	mean hepatocyte volume (μm^3)
$V_v$cyt	volume fraction occupied (in a volume of parenchyma) by hepatocyte cytoplasm
$V_v$end	volume fraction occupied (in a volume of parenchyma) by endothelia
$V_v$extra	volume fraction occupied (in a volume of liver) by extraparenchymal components (centrilobulars veins, portal triads, Glisson capsule)
$V_v$hep	volume fraction occupied (in a volume of parenchyma) by hepatocytes
$V_v$nuc	volume fraction occupied (in a volume of parenchyma) by hepatocyte nuclei
$V_v$par	volume fraction occupied (in a volume of liver) by liver parenchyma
$V_v$sin	volume fraction occupied (in a volume of parenchyma) by sinusoidal lumen

an interactive approach on an image analyser (Kontron-Zeiss KS300) with software specially tailored to the research needs by our team. The analyser automatically superimposed on each microscopic field displayed on the monitor different grids of points and lines included in a test area of 504×504 pixels, allowing stereological parameter evaluation.

The observer was able to apply interactive techniques of enhancement for better definition of cellular structures. It was also possible to exclude fields too damaged for analysis. A total of 15–20 microscopic fields, systematically selected, were examined for each section (1 section per block, 5 blocks per case). For each case the analysed area therefore corresponded to ~ 250000–350000 μm².

MORPHOMETRIC MODEL

The adopted model requires the determination of parameters suitable for the morphometric characterisation of liver (De Hoff & Rhines, 1968; James, 1977). These are listed in Table 2.

Volumetric analyses were performed by differential point counting (De Hoff & Rhines, 1968; Delesse, 1847) and surface densities evaluated by differential intersection counting (Elias et al. 1971). The size distribution and number in unit volume were derived by diameter analysis according to the Schwartz-Saltykov method (Saltykov, 1967), modified after De Hoff (Staubli et al. 1969).

BIOCHEMICAL AND CLINICAL PARAMETERS

Over 200 biochemical and clinical parameters have been evaluated. Statistical analysis (correlation analysis) showed significance for the following variables: (1) warm ischaemia time (Iw); (2) maximum value of aspartate transferase during first week post-OLT (AST); (3) maximum value of alanine transferase

Table 2. *Morphometric parameters used*

Volume fractions occupied by:
- liver parenchyma ($V_v$par),
  - hepatocyte cytoplasm ($V_v$cyt)
  - hepatocyte nuclei ($V_v$nuc)
  - sinusoidal lumen ($V_v$sin)
  - endothelium (sinusoidal endothelial cells, Ito cells, Disse space included) ($V_v$end)

Extraparenchymal components (centrilobular veins, portal triads, Glisson capsule) ($V_v$extra)

Surface densities of:
- parenchymal sides of hepatocytes (i.e. sides facing neighbouring hepatocytes) ($S_v$par)
- vascular sides of hepatocytes (i.e. sides exposed to Disse space) ($S_v$vas)
- sinusoidal bed (i.e. sides exposed to sinusoidal blood flow) ($S_v$sin)

Number in unit volume and size distribution of hepatocyte nuclei as representative of mononucleated hepatocytes (N_v)

Mean hepatocyte nuclei diameter ($\bar{d}_{nuc}$)

Mean hepatocyte diameter ($\bar{d}_{hep}$) and volume ($\bar{V}$)

Hepatocyte nucleus/cytoplasm ratio, N/C.

Table 3. *Main morphometric parameters evaluated at each time point**

	Dimension	T1	T2	T3
$V_v$par	mm^3/mm^3	0.8295 ± 0.0496	0.8463 ± 0.0427	0.8612 ± 0.0440
$V_v$cyt	mm^3/mm^3	0.7888 ± 0.0412	0.7890 ± 0.0366	0.7869 ± 0.0615
$V_v$nuc	mm^3/mm^3	0.0433 ± 0.0067	0.0454 ± 0.0106	0.0457 ± 0.0056
N/C	mm^3/mm^3	0.0523 ± 0.0088	0.0544 ± 0.0121	0.0555 ± 0.0100
$V_v$sin	mm^3/mm^3	**0.0362 ± 0.0184***	**0.0479 ± 0.0187°**	**0.0373 ± 0.0221***
$V_v$end	mm^3/mm^3	**0.1318 ± 0.0343***	**0.1176 ± 0.0368°**	**0.1300 ± 0.0434***
$V_v$extra	mm^3/mm^3	0.1656 ± 0.0367	0.1654 ± 0.0313	0.1637 ± 0.0581
$S_v$par	mm^2/mm^3	**92.6044 ± 14.7229***	**90.4505 ± 17.2765°**	**95.3433 ± 16.4296^**
$S_v$sin	mm^2/mm^3	**12.9456 ± 6.2227***	**17.6717 ± 6.7678°**	**11.5755 ± 4.6260***
$S_v$vas	mm^2/mm^3	**50.9535 ± 9.2428***	**51.6181 ± 6.4429***	**43.6770 ± 9.3896°**
N_v	$1/mm^3$	**$143{,}766 \pm 32{,}239$***	**$139{,}411 \pm 24{,}7211$°**	**$135{,}437 \pm 39{,}003$^**
$\bar{d}_{nuc}$	μm	7.78 ± 1.15	7.81 ± 1.09	8.11 ± 1.10
$\bar{d}_{hap}$	μm	22.53 ± 1.94	22.67 ± 1.37	23.05 ± 2.15
$\bar{V}$	μm^3	**6117.85 ± 1603.95***	**6161.48 ± 1099.61***	**6565.16 ± 1642.18°**

* All results are given as mean ± S.D. When 2-way ANOVA showed differences between time points, the Scheffé post-hoc test was performed: for these parameters (in bold type) different symbols *°^ mark mean values that are significantly different ($P < 0.05$). No symbols are used for parameters not significantly varying between time points.

Table 4. *Correlation matrix**

	$V_v$nuc	$V_v$hep	N/C	$V_v$sin	$V_v$extr	$V_v$par	$S_v$par	$S_v$vas	$S_v$sin	N_v	$\bar{V}$	$\bar{d}_{hep}$	$\bar{d}_{nuc}$
$V_v$cyt	**−0.1575** 0.007	**0.9845** 0.000	**−0.4793** 0.000	**−0.4532** 0.000	**−0.8032** 0.000	**0.3462** 0.000	**0.1560** 0.008	**−0.4186** 0.000	**−0.2695** 0.000	**−0.5124** 0.000	**0.6093** 0.000	**0.6301** 0.000	**0.3932** 0.003
$V_v$nuc		0.0182 0.758	**0.9362** 0.000	−0.0017 0.977	0.0701 0.233	−0.0163 0.785	**0.2192** 0.000	0.0816 0.167	0.0138 0.815	0.3091 0.020	−0.2763 0.040	−0.2815 0.036	0.2413 0.074
$V_v$hep			**−0.3189** 0.000	**−0.4591** 0.000	**−0.8014** 0.000	**0.3472** 0.000	**0.1969** 0.001	**−0.4094** 0.000	**−0.2704** 0.000	**−0.4722** 0.000	**0.5773** 0.000	**0.5984** 0.000	**0.4482** 0.001
N/C				**0.1607** 0.006	**0.3371** 0.000	−0.1350 0.022	**0.1611** 0.006	**0.2097** 0.000	0.0978 0.098	**0.4491** 0.001	**−0.4375** 0.001	**−0.4542** 0.000	**0.0761** 0.580
$V_v$sin					**0.5804** 0.000	**−0.2683** 0.000	0.1088 0.065	**0.3201** 0.000	**0.7803** 0.000	0.2871 0.032	−0.3165 0.018	−0.3373 0.011	−0.1782 0.188
$V_v$extra						**−0.4582** 0.000	−0.1511 0.010	**0.5424** 0.000	**0.3963** 0.000	**0.5172** 0.000	**−0.5863** 0.000	**−0.6134** 0.000	**−0.4645** 0.000
$V_v$par							**0.1750** 0.003	**−0.3071** 0.000	−0.0882 0.138	**−0.3625** 0.006	**0.3612** 0.006	**0.3865** 0.003	**0.4302** 0.001
$S_v$par								**−0.2603** 0.000	**0.1691** 0.004	0.2283 0.092	−0.1072 0.432	−0.123 0.348	0.2671 0.047
$S_v$vas									**0.3959** 0.000	**0.4213** 0.001	**−0.5251** 0.000	**−0.5214** 0.000	−0.2254 0.096
$S_v$sin										0.0901 0.508	−0.1745 0.201	−0.1632 0.231	0.0854 0.532
N_v											**−0.9505** 0.000	**−0.9723** 0.000	**−0.5531** 0.000
$\bar{V}$												**0.9944** 0.000	**0.5813** 0.000
$\bar{d}_{hep}$													**0.5874** 0.000

* For each cell, bivariate correlation coefficients (Pearson) and probability values (2-tailed) are given. Significant correlations (at the 0.01 level) are in bold type. *P* values are rounded to the third decimal place ($P = 0.000$ means $P < 0.0005$).

during first week post-OLT (ALT); minimum value of platelets during first week post-OLT (PLT); (4) maximum value of biliary flux during first week post-OLT (Bfmax); (5) minimum value of biliary flux during first week post-OLT (Bfmin); (6) maximum value of serum total bilirubin during first week post-OLT (Bil); and (7) minimum value of prothrombin time during first week post-OLT (PT). For all patients enrolled in the study, the follow-up status was recorded.

STATISTICAL ANALYSIS

Comparison among time points was performed for each parameter, by variance analysis with factorial design followed by the Scheffé post-hoc test (Snedecor & Cochran, 1972; Armitage, 1973); in addition, a correlation matrix has been evaluated. Cluster analysis (Anderberg, 1973) has been performed for biochemical and clinical parameters. Finally, correlation analysis was undertaken between the morphometric parameters and clusters obtained from analysis of the biochemical/clinical data.

RESULTS

Table 3 shows the mean values, with the relevant standard deviations, of the morphometric parameters at each time point, and Table 4 the matrix of correlation referred to all morphometric parameters; statistically significant coefficients are given in bold type. Table 5 shows the classes related to the cluster analysis performed on the biochemical and clinical data. According to these parameters, liver transplant recipients cluster into 3 classes: cluster 1, patients with

Table 5. *Cluster analysis**

	Cluster 1	Cluster 2	Cluster 3
Number of patients	4§	5°	11^
Iw (h)	1.65	2.13	1.64
AST (IU/L)	1334.5	6296	1316
ALT (IU/L)	945.25	4630	1005.09
PLT (*1000/ml)	46.50	25.0	33.75
Bfmax (ml/24 h)	156.75	56.6	127.91
Bfmin (ml/24 h)	60	9	47.18
Bil (mg/l)	19.58	26.16	18.3
PT (%)	44	16.2	41.73

* This identified 3 clusters that describe the transplant population according to biochemical and clinical data. Each cluster describes, in terms of the data collected, the class to which the patients submitted to OLT belong. The 3 classes represent patients with respectively unremarkable clinical course (cluster 1), rapidly life-threatening clinical course (cluster 2) and complicated clinical course (cluster 3).

§ One patient died on d 53 post-OLT from multi-organ failure; ° 2 patients died respectively on d 7 and d 11 post-OLT from primary graft dysfunction; 3 patients were submitted to hepatic retransplantation as a consequence of primary graft dysfunction; ^ 4 patients died on the first month post-OLT from complications other than those related to liver transplantation.

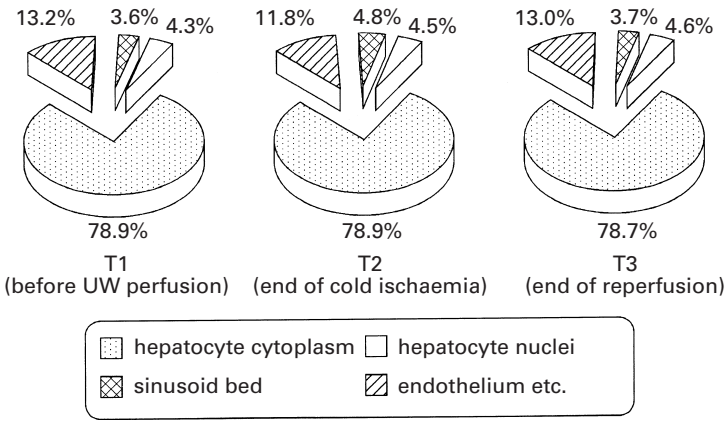

Fig. 1. Liver parenchyma. Volume fractions of chief parenchymal components, evaluated by differential point counting, at the 3 time points which best identify cold ischaemia and warm ischaemia/reperfusion spans. Each component is given as a percentage of parenchymal volume.

Table 6. *Mean values of the morphometric parameters correlated with each cluster for each time point*

	Cluster 1	Cluster 2	Cluster 3
$V_v$sin T1	0.1450	0.1221	0.1322
T2	0.1269	0.1040	0.1192
T3	0.1539	0.1029	0.1368
$V_v$end T1	0.0332	0.0354	0.0326
T2	0.0467	0.0492	0.0479
T3	0.0268	0.0292	0.0433
$S_v$par T1	118.72	130.99	130.70
T2	106.07	126.89	129.40
T3	103.06	121.17	138.36
$S_v$sin T1	14.97	17.90	16.36
T2	20.98	26.85	24.44
T3	10.17	15.18	17.43
$S_v$vas T1	70.13	69.67	67.33
T2	72.70	67.91	71.06
T3	61.61	53.47	62.31
N_v T1	161819	139732	133518
T2	138951	138354	139962
T3	118811	133946	139795
$\bar{d}_{hep}$ T1	21.47	22.94	23.07
T2	22.52	22.90	22.64
T3	23.62	23.39	22.78

an unremarkable clinical course; cluster 2, patients with a rapidly life-threatening clinical course and, finally, cluster 3, patients with a complicated clinical course. Table 6 shows the correlation between the mean values of the morphometric parameters at each time point and the clusters related to the biochemical and clinical data.

Figure 1 gives pie charts with the volume fractions of the different parenchymal components at each time point. Data referred to the volume fraction of nuclei ($0.0433 \rightarrow 0.0454 \rightarrow 0.0457$) and cytoplasm ($0.7888 \rightarrow 0.7890 \rightarrow 0.7869$) of the hepatic cells show no significant alteration.

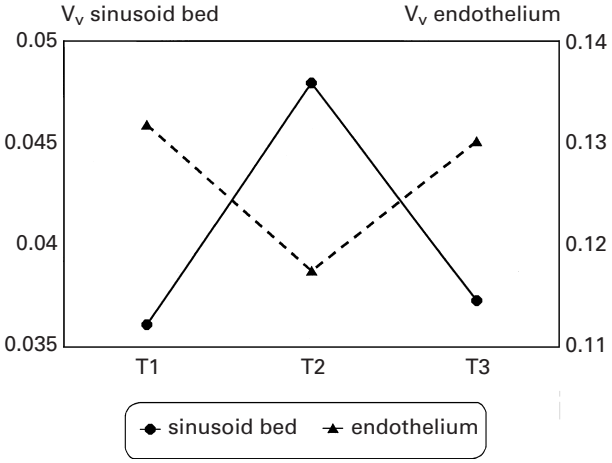

Fig. 2. Sinusoidal compartment. Volume fractions of endothelium (Disse space, Kupffer and Ito cells included, left scale) and of sinusoids lumen (right scale) are plotted at the 3 time points T1, T2 and T3 (see legend to Fig. 1).

Figure 2 shows the trend of the sinusoid bed during I/R phases. To underline the association between morphometric parameters referred to the same morphological characteristic, 2 parameters have been given in the graph, both related to the sinusoid bed. The volume fractions of the sinusoid district components, $V_v$end ($0.132 \rightarrow 0.118 \rightarrow 0.130$) and $V_v$sin ($0.0362 \rightarrow 0.0479 \rightarrow 0.0373$) appear to show relevant and opposite 'movements' during ischaemia/reperfusion phases.

Figure 3 illustrates the findings for the surface of the hepatocytes (represented by each pie chart) and shows the variations of the ratio between the parenchymal and vascular sides, the former facing the sinusoids and space of Disse and the latter facing neighbouring hepatocytes. The parameters are, respectively, the surface densities of parenchymal sides, $S_v$par ($92.60 \rightarrow 90.65 \rightarrow 95.34$ mm^2/mm^3), and of vascular sides, $S_v$vas ($50.95 \rightarrow 51.61 \rightarrow 43.67$ mm^2/mm^3).

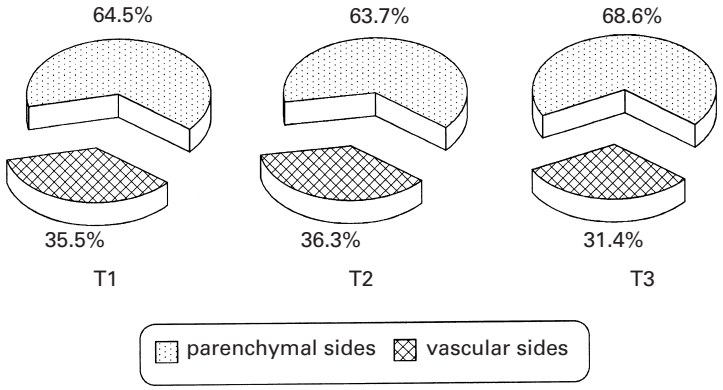

Fig. 3. Hepatocyte surface. Each pie chart represents the surface of hepatocytes, and shows the surface percentage represented respectively by parenchymal and vascular sides, the former facing sinusoids and space of Disse, the latter facing neighbouring hepatocytes. Time points are the same as in Figs 1 and 2.

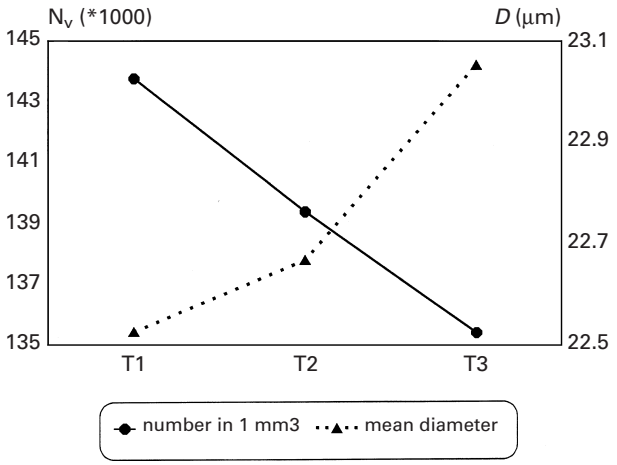

Fig. 4. Hepatocytes. Number of hepatocytes per unit volume (left scale, *1000) and mean hepatocyte diameter (right scale) are plotted at the same time points as in the other figures.

Figure 4 gives the trend during ischaemia/reperfusion phases of the mean number of hepatocytes per unit test volume (N_v: $143.770 \rightarrow 139.410 \rightarrow 135.440$ per mm³) and, reciprocally, of the mean size of hepatocytes ($\bar{d}_{hep}$: $22.53 \rightarrow 22.67 \rightarrow 23.05$ μm).

DISCUSSION

The deprivation of hepatic blood inflow and the restoration of warm oxygenated blood during OLT may lead to the generation of oxygen free radicals, derangement of calcium and mitochondrial homeostasis and lipid membrane peroxidation.

During I/R phases (Fig. 1) the volume fraction of hepatocytes (nucleus and cytoplasm) shows no prominent modifications; it is the capillary district that is mainly involved. We observed that the endothelial volume fraction at the end of cold ischaemia is decreased ($V_v$end: from 0.132 to 0.118). After reperfusion, endothelial volume is significantly increased and almost achieves the same values as at the beginning of ischaemia ($V_v$end from 0.118 to 0.130).

The sinusoidal bed shows opposite modifications when compared with the endothelium (Fig. 2): it exhibits a significant peak value at the end of cold ischaemia, returning to baseline values at the end of the reperfusion ($V_v$sin: $0.33 \rightarrow 0.48 \rightarrow 0.37$).

The vascular compartment (the sum of $V_v$end plus $V_v$sin) is not significantly modified during I/R because the endothelium/sinusoid-bed ratio is reciprocally inverted at the end of cold ischaemia when sinusoidal bed volume is increased and the endothelial volume fraction is decreased. These data are probably the consequence of damage of the endothelial cells, but they could also be related to the characteristics of the preservation solution (pressure, temperature and composition of UW).

At the end of liver transplantation (third biopsy) the alteration of the vascular compartment reflects the effects of warm ischaemia/reperfusion: the endothelium swells, thus reducing the volume fraction of the sinusoid bed. These modifications represent the progression of endothelial injury (McEon et al. 1988; Caldwell-Kenkel et al. 1989).

The volume fraction of hepatocytes does not seem to be influenced by I/R (Fig. 1), but the hepatic cell is not insensitive to this sequence of events, showing a rearrangement of its surface profile (Fig. 3). We observed at the second biopsy that the surface density of the vascular side is significantly increased ($S_v$vas: from 50.95 to 51.62 mm²/mm³); conversely, the same parameter referred to the parenchymal sides shows a marked decrease ($S_v$par: from 92.60 to 90.65 mm²/mm³). This profile alteration is probably dependent upon an insufficient delivery of oxygen and blood flow during the ischaemic phase and could

represent an adaptive defensive mechanism by the hepatic cell. The architectural changes of the hepatic cells show a severe alteration at the third biopsy: reperfusion of the ischaemic liver leads to a further modification of cell profiles. The parenchymal sides are increased ($S_v$par: from 90.65 to 95.34 mm^2/mm^3) while the vascular sides are sharply reduced ($S_v$vas: from 51.62 to 43.68 mm^2/mm^3). This structural modification could be the consequence of cell damage. Nevertheless, an adaptive mechanism could justify the reduction of the surface exposed to a subendothelial space that is characterised by low pH and high levels of toxic metabolites.

Two other morphometric parameters related to hepatocytes show an interesting trend. The number of hepatocytes per unit volume decreases (N_v: $143.770 \rightarrow 139.410 \rightarrow 135.440$ per mm^3); these data can be related to the death of some parenchymal cells together with a slight increase in hepatocyte diameter during postischaemic reperfusion ($\bar{d}_{hep}$: $22.53 \rightarrow 22.67 \rightarrow 23.05$ μm). This increased diameter of hepatocytes could explain, at least in part, the liver swelling which occurs during ischaemia.

Figure 4 clearly shows a reduced number of hepatocytes with a larger surface. The increased hepatocyte diameter and the reduced number of hepatocytes per mm^3 suggest that some hepatocytes have been killed during the different steps of liver grafting, although we did not investigate hepatocellular necrosis. This hypertrophic phase cannot be simply interpreted as an adaptive reaction to ischaemic injury. Previous studies (Vizzotto et al. 1986, 1989) have reported an early hyperplastic phase with a burst of mitosis among cells standing by in phase G_0 during liver regeneration after hepatectomy in rats; at the same time point the sinusoid bed was enlarged. The authors also stressed that the increased surface density of vascular sides represents a good indicator of the better trophic condition of the hepatocytes during liver regeneration.

In our study this hyperplastic phase is not (probably not yet) present at the end of I/R and the morphometric fluctuations parallel the increasing metabolic stress during the transplant procedure. The decrease of morphometric parameters referred to the sinusoid district has also been described in the liver of castrated rats, where the trophic and hyperplastic influence of testosterone is absent (Vizzotto et al. 1996).

The fluctuations of vascular and parenchymal components, which are involved in the reactions during I/R, occur with a definite characteristic temporal course: the injury of sinusoid cells, which provide a graded barrier between the sinusoid lumen and the space of Disse, affects hepatocyte function, particularly during warm ischaemia and reperfusion. In particular, the extent of the modifications of hepatic cell profiles during I/R, showed here for the first time, could represent an alternative morphological index to evaluate the degree of cellular injury and so be helpful for a better comprehension of the mechanisms involved in ischaemia/reperfusion alterations.

It is important to point out that these structural modifications, which are undoubtedly the basis for functional impairment, are not large enough to be observed qualitatively, only morphometric analysis leading to statistically significant differences.

For each patient we have collected biochemical and clinical data during the transplantation procedure and the first posttransplant week. Using cluster analysis, patients have been sorted into the 3 classes: uneventful clinical course (4 patients, cluster 1), rapid worsening clinical course (5 patients, cluster 2) and complicated clinical course (11 patients, cluster 3). For each time point, mean values for the morphometric parameters significantly different on statistical analysis have been correlated for each cluster (Table 6). It is noteworthy that in cluster 1, $V_v$end shows a decrease during the ischaemia phase and a significant increase at the end of reperfusion. Conversely, cluster 2 is characterised by a marked decrease of the endothelial volume fraction both during the ischaemia and reperfusion phases.

In cluster 1, N_v is decreased at the end of I/R, while hepatocyte diameter is increased at the end of reperfusion. On the other hand, in the other 2 clusters these 2 parameters are only slightly altered during I/R. Also, the surface density of hepatocytes (the sum of N_v and $\bar{d}_{hep}$) is unchanged in clusters 1 and 3 during I/R while it decreases in cluster 2. Finally, in cluster 1 the percentage of $S_v$vas at the end of reperfusion reaches the same values as at the beginning of ischaemia, while in clusters 2 and 3 it shows a marked decrease at the end of the I/R phases.

Two points must be emphasised. The first is that cluster 1 is characterised by adaptive mechanisms during I/R phases, while the other 2 clusters (this is particularly true for cluster 2) show a quite reduced response during I/R phases. The second point is related to the morphometric parameters and their relationship with biochemical and clinical data. It is noteworthy that the 3 clusters show relevant differences at the first biopsy. These data can reflect the influence of features which are directly related to the donor (i.e. intensive care unit stay, administered drugs) and which may cause, at least in part, a

condition of functional susceptibility of the liver to the insult occurring during I/R. According to our results, morphometric analysis seems to identify morphological parameters which can be useful predictive indicators of graft function. These observations indicate that more attention must be given to the status of the donor, which may presumably influence the outcome of OLT. However, it would be premature to consider these structural morphometric data as absolute prognostic indicators in liver transplantation. Other studies on a large series including much longer cold preservation times and marginal liver donors are needed.

REFERENCES

ANDERBERG MR (1973) *Cluster Analysis for Applications*. New York: Academic Press.

ARMITAGE P (1973) *Statistical Methods in Medical Research*, pp. 147–166. Oxford: Blackwell Scientific.

CALDWELL-KENKEL JC, CURRIN RT, TANAKA Y, THURMAN RG, LEMASTERS JJ (1989) Reperfusion injury to endothelial cells following cold storage of rat liver. *Hepatology* **10**, 292–299.

CLAVIEN PA, HARVEY PR, STRASBERG SM (1992) Preservation and reperfusion injuries in liver allografts. *Transplantation* **53**, 957–978.

CUTRIN JC, CANTINO D, BIASI F, CHIARPOTTO E, SALIZZONI M, ANDORNO E et al (1996) Reperfusion damage to the bile canaliculi in transplanted human liver. *Hepatology* **24**, 1053–1057.

DE HOFF RT, RHINES FN (1968) *Quantitative Microscopy*. New York: McGraw-Hill.

DELESSE A (1847) Procédé méchanique pour déterminer la composition des roches. *Paris: Compte Rendu de L'Académie des Sciences D* **51**, 544–567.

ELIAS H, HENNING A, SCHWARTZ DE (1971) Stereology: applications to biomedical research. *Physiological Reviews* **51**, 158–200.

ENGERSON TD, McKELVEY T, RHYNE DB, BOGGIO EB, SNYDER SJ, JONES HP (1987) Conversion of xanthine dehydrogenase to xanthine oxidase in ischemic rat tissue. *Journal of Clinical Investigation* **79**, 1564–1570.

GRACE PA (1994) Ischaemia-reperfusion injury. *British Journal of Surgery* **81**, 637–647.

HESS FA, GNAEGI HR, WEIBEL ER, PREISIG R (1973) Morphometry of dog liver: comparison of wedge and needle biopsies. *European Journal of Clinical Investigation* **3**, 451–458.

JAESCHKE H (1991) Vascular oxidant stress and hepatic ischemia/reperfusion injury. *Free Radical Research* **12–13**, 737–743.

JAESCHKE H, FARHOOD A (1991) Neutrophil and Kupffer cell-induced oxidant stress and ischemia-reperfusion injury in rat liver. *American Journal of Physiology* **260(3 pt 1)**, G355–62.

JAMES NT (1977) Stereology. In *Analytical and Quantitative Methods in Microscopy* (ed. Meek GA, Elder HY), Cambridge: Society for Experimental Biology Seminar Series, Cambridge University, pp. 9–28.

KALAYOGLU M, SOLLINGER HW, STRATTA RJ, D'ALESSANDRO AM, HOFFMANN RM, PIRSCH JD et al (1988) Extended preservation of the liver for clinical transplantation. *Lancet* **1(8586)**, 617–619.

KARWINSKI W, GARCIA R, SCOTT HELTON W (1996) Protective effects of the calcium channel blocker verapamil on hepatic function following warm ischemia. *Journal of Surgical Research* **64**, 150–155.

McCORD JM (1985) Oxygen derived free radicals in post-ischemic tissue injury. *New England Journal of Medicine* **312**, 159–163.

McEON CMB, EDWARDS V, PHILLIPS MJ, HARVEY PRC, PETRUNKA CN, STRASBERG SM (1988) Sinusoidal lining cell damage: critical injury in cold preservation of liver allografts in the rat. *Transplantation* **46**, 187–191.

MUELLER AR, PLATZ KP, HAAK M, UNDI H, MULLER C, KOTTGEN E et al. (1996) The release of cytokines, adhesion molecules, and extracellular matrix parameters during and after reperfusion in human liver transplantation. *Transplantation* **62**, 1118–1126.

OBERHOLZER M, ROHR HP (1983) Liver morphometry. In *A Manual of Morphometry in Diagnostic Pathology* (ed. Baak JPA, Oort J), pp. 126–131. Berlin: Springer.

REILLY PM, BULKLEY GB (1990) Tissue injury by free radicals and other toxic oxygen metabolites. *British Journal of Surgery* **77**, 1324–1325.

SALTYKOV SA (1967) A stereological method for measuring the specific surface area in metallic powders. In *Stereology* (ed. Elias H), pp. 63–64. Berlin: Springer.

SCOAZEC JY, BORGHI-SCOAZEC G, DURAND F, BERNUAU J, PHAM BN, BELGHITI J et al. (1997) Complement activation after ischemia-reperfusion in human liver allografts: incidence and pathophysiological relevance. *Gastroenterology* **112**, 908–918.

SNEDECOR GW, COCHRAN WG (1972) *Statistical Methods*, pp. 135–171. Ames, Iowa: Iowa State University Press.

SOUTHARD JH, VAN GULLK TM, AMETANI MS, VREUDGENHIL PK, LINDELL SL, PIENAAR BL et al. (1990) Important components of the UW solution. *Transplantation* **49**, 251–257.

STAUBLI W, HESS R, WEIBEL ER (1969) Correlated morphometric and biochemical studies on the liver cell. *Journal of Cell Biology* **42**, 92–112.

VIZZOTTO L, ASENI P, ROMANI F, FERRARIO VF, BEATI C, TOMMASINI DEGNA C (1986) Liver regeneration: a semicomputerised morphometric model [Abstract]. *Journal of Hepatology* **1**(Suppl), S1.

VIZZOTTO L, ROMANI F, FERRARIO VF, TOMMASINI DEGNA C, ASENI P (1989) Characterization by morphometric model of liver regeneration in rat. *American Journal of Anatomy* **185**, 445–454.

VIZZOTTO L, VERTEMATI M, MARINELLO E, LEONCINI R, PAGANI R, PIZZICHINI M (1996) Effect of testosterone on purine metabolism and morphometric parameters in the rat liver. *Molecular & Cellular Endocrinology* **119**, 123–128.